Development of a 50 kW Wireless Power Transfer System

Alex Ridge, Ku Ku Ahamad, Richard McMahon
WMG, University of Warwick
Coventry, UK
a.ridge@warwick.ac.uk

John Miles
Dept. of Engineering,
University of Cambridge
Cambridge, UK

***Abstract*—A high-power modular wireless power transfer system has been developed intended for use in larger vehicles. This paper presents the design methodology and evolution of the system, including test results. The system utilises SiC switching devices and an 85 kHz operating frequency. 50 kW of wireless power transfer has been achieved over a 200 mm gap at 89% efficiency, showing good promise for the system.**

***Index Terms*—Wireless power transfer, inductive power transfer, modelling, optimisation, experimental results, Silicon Carbide**

I. Introduction

In recent years, environmental pressures and air quality concerns have led to a reconsideration of transport technologies. The emergence of electric vehicles (EVs) as a solution to these concerns has been very significant and is an area of active development both in research and commercial spheres. The introduction of EVs however poses a number of challenges particularly around vehicle range and charging.

When applied to the charging of EVs, wireless power transfer (WPT) systems can offer advantages over conventional cable-based charging in terms of convenience, automation, safety and physical robustness of EV charging infrastructure. WPT systems are actively being developed for this use [1].

One application of high-power WPT systems is in electric buses. The issue of tailpipe emissions from diesel vehicles in city centres is one of particular recent concern, prompting a shift towards electric buses for passenger transport in cities. High-power WPT systems can enable convenient opportunity charging schemes for electric buses, topping up the battery on the bus during short periods when the bus is stationary at a bus stop. Regular opportunity charging through the day enables buses to be designed with lower capacity batteries, a proposition which is likely to be attractive to bus operators as the associated saving in battery weight can lead to increased passenger-carrying capacity of the bus.

Other applications of WPT include implementation in parking spaces where convenience is attractive, and charge-on-the-move systems where cable connections are not practical.

In recent decades the development of power semiconductor devices (both Silicon (Si) devices and in recent years Silicon Carbide (SiC) devices) has opened the door for the efficient realisation of WPT systems [2].

The system under consideration has been developed towards the requirements of large EVs (such as buses and trucks) but can also be applicable to smaller EVs. It aims to transfer significant power over the full distance from the road surface to the EV (i.e. without the need for mechanical articulation of system components). A modular approach has been adopted, such that the system can be scaled for different sizes and power-requirements of EVs. A relatively thin module width has been chosen to assist integration within a vehicle chassis.

II. Design

A. Operating frequency

Operating frequency is a key consideration in the design of any WPT system. For a given WPT system electromagnetic configuration, the power that can be transferred through system is proportional to the operating frequency. However, higher operating frequencies pose greater challenges for the power electronics driving the WPT system as they can lead to increased switching losses, ferrite losses and potentially large driving voltages for the coils due to the coil inductance. Earlier WPT systems commonly operated at a frequency of around 20 kHz. With recent advances in power electronics, newer systems commonly operate at 85 kHz. The newest guidance for light-duty electric vehicles (SAE J2954 [3]) sets a frequency range of 81.38 to 90 kHz for IPT systems. Whilst SAE J2954 considers modules up to 22 kW rating (with higher power module requirements only provisionally defined), the same 85 kHz frequency is chosen here for consistency with existing standards. In the future, even higher operating frequencies may be attractive.

B. Electromagnetic pad topology and system modularity

A number of different types of pad topology have been proposed in literature and also implemented in practice. In general, single-sided pad topologies were considered preferable as they encourage magnetic flux to flow on predominantly one side of the pad, inherently increasing the potential for magnetic coupling and reducing the requirement for shielding.

Within single-sided pad topologies, common topologies include circular pads and various types of bipolar pads. For a given outer dimension, bipolar pad designs can exhibit effective coupling over greater airgaps than circular pads and hence were attractive for this large airgap application [4], [5].

Additionally, in bipolar pad designs the magnetic flux path is orientated predominantly along the length of the pad (vs radially around the pad in circular designs), and furthermore the length and width of the pad can be adjusted independently to one another. These characteristics are ideally suited to the desire for a relatively thin and compact electromagnetic pad. Considering the potential for stray field around the module, the predominant flux direction can be aligned for best integration within / near a vehicle chassis. It is anticipated that the most likely orientation is for the length of the pad to be aligned with the length of the vehicle. For the system constructed here, a 'DD' pad topology was chosen in which the two coils in the pad are always operated in antiphase to one another so as to effectively channel the magnetic flux [4].

For a given available space underneath a vehicle, a trade-off exists between the number of modules and the 'aspect ratio' (airgap vs pad dimensions) of the flux path. A larger number of modules gives greater potential flexibility in terms of module placement and system adaptability to different power requirements, but would lead to reduced module dimensions and potentially poorer electromagnetic coupling over a given airgap. A system consisting of a small number of higher-power modules was chosen to allow for suitable length per module to be realised whilst maintaining the attractiveness of a modular system.

C. Modelling and optimisation

In order to design and optimise the pads for this application, a finite element (FEA) application was used. For initial development and FEA model validation, a small set of pads was developed (Fig. 1). These pads were of a 'DD'-type topology and approximately the size of an A4 sheet. The coils are constructed using Litz wire, backed by N87 ferrite strips. The pads are housed in laser-cut acrylic and positioned nominally 40 mm apart.

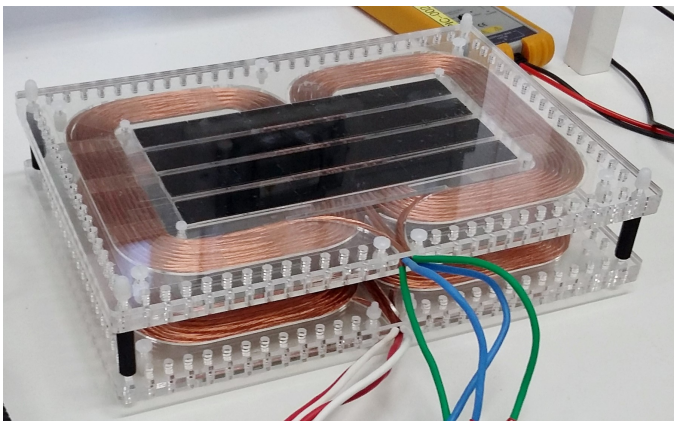

Fig. 1. Photo of small prototype WPT pads

A comparison is given in Table I of the coupling and inductance parameters from FEA simulation vs those measured experimentally. The difference is within 5 % which is reasonable. It was noted from the simulations that there was some sensitivity of the parameters to any spacing between the ferrite sub-blocks that make up the strips, and this may account for some of the variation observed.

TABLE I
SMALL WPT PADS PARAMETERS COMPARISON

Parameter	Measured	Simulated	Difference (%)
Primary pad inductance (L_A)	81.9 uH	83.7 uH	2
Secondary pad inductance (L_B)	79.3 uH	83.7 uH	5
Coupling coefficient (k)	0.47	0.48	2

Further tests were conducted on the small pads to confirm the transfer of power. For these tests the primary pad was compensated with an LCL compensation network and the secondary pad was simply parallel-compensated. The primary side was driven by a small H-bridge inverter developed for the purpose, fed from a DC source. The secondary side was loaded with a resistor. For these initial tests on the small pads, an operating frequency of 20 kHz was used.

The results from this test are shown in Table II. Also shown in Table II is the comparison to a simulation of the circuit constructed in MATLAB Simulink®. There is good agreement here also. These results provide confidence in the modelling and simulation efforts.

TABLE II
SMALL WPT PADS POWER TEST RESULTS

Parameter	Measured	Simulated	Difference (%)
Primary pad voltage	27.5 Vrms	28.9 Vrms	5
Primary pad current	2.8 Arms	2.9 Arms	3
Load current	1.17 Arms	1.21 Arms	3
Output power	61.5 W	65.7 W	6

Following this exercise, the FEA models for full-sized pads were explored and optimised with the primary aim of achieving high coupling coefficient (k) between the two pads. For speed of simulation, a linear model was used for the Ferrite – this assumes the ferrite is operating in the linear region (which is generally the aim for WPT systems so as to avoid excessive ferrite losses) however this must be checked for a final design. If required, the ferrite thickness can be adjusted to give a suitable flux density without significantly affecting other modelling results.

The base starting point for the optimisation (shown in Fig. 2) already incorporated several useful design features:

1) A 'reduced ferrite' topology in which the ferrite within each module is comprised of several strips rather than a solid plate. This helps trade off module weight and cost against performance.
2) Semi-pancake coils in which the turns of wire lie flat against the ferrite in the middle of each pad (where they cross the ferrite) but are bunched as they loop round the ferrite. This helps reduce pad width compared to a pure pancake coil by reducing the width of the coils on the

sides of the module, improving module performance for a given set of dimensions.

3) Vertical ferrite extensions in the middle of each coil. This brings the backing ferrite flush with the coil surface, increasing the coupling coefficient while not affecting the air gap.

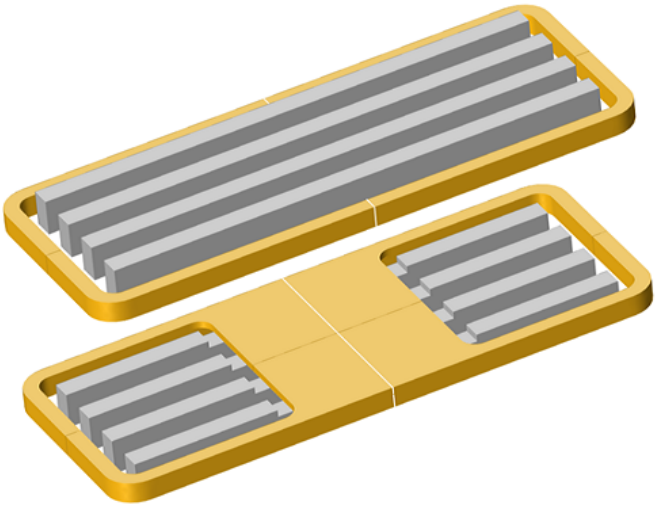

Fig. 2. Base FEA model (grey = ferrite, orange = copper area)

A number of aspects were explored during the optimisation stage, including ferrite arrangement, coil / ferrite spacing, coil coverage of ferrite in the central portion of coils, and bunching of coils to make best use of the available area for the pads. The resulting pads are approximately 0.75 m long and 0.3 m wide with an airgap of 200 mm. The key electrical characteristics of the pads are listed in Table III along with measured results, which show reasonable agreement (within 9 %).

TABLE III
FULL-SIZE WPT PADS PARAMETERS COMPARISON

Parameter	Measured	Simulated	Difference (%)
Primary pad inductance	12.4 uH	12.1 uH	3
Secondary pad inductance	12.4 uH	12.1 uH	3
Coupling coefficient (k)	0.21	0.23	9

D. Circuit modelling and optimisation

Having explored the best electromagnetic design for the pads, attention was turned to the circuits that will power them. A number of resonant circuit designs exist in the literature. The chosen topology was an LCC resonance circuit as is often common where tolerance to load changes and misalignment is desirable [6], [7]. On the secondary side, a similar compensation circuit was used. The output from the secondary compensation circuit was passively rectified into a DC link. Passive rectification helps minimise the complexity of any on-vehicle electronics and was the preferred method at this time, with power control in the system from the primary side. The trade-off between increased system complexity versus potential extra control flexibility associated with the integration of active components into the secondary side may be examined in more detail in the future. The circuits were modelled in Simulink and both bode plots and time-domain simulations were used to optimise the circuit parameters. The aim was for the system to appear slightly inductive and the inverter output to facilitate zero voltage switching (ZVS) of the inverter, as well as to deliver the required power. During the optimisation process, the 'L' on the secondary side was eliminated as this was found to produce the best results. The resulting circuit is shown in Fig. 3.

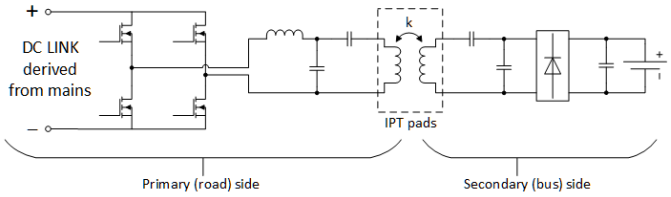

Fig. 3. System circuit

III. SYSTEM CONSTRUCTION

The pads were constructed from two coils of Litz wire (to make a DD configuration) and a series of ferrite strips, embedded in a wooden holder. These pads are intended for lab use. For simplicity, shielding was omitted at the time of construction and for these initial tests. The resulting WPT pads are shown in Fig. 4.

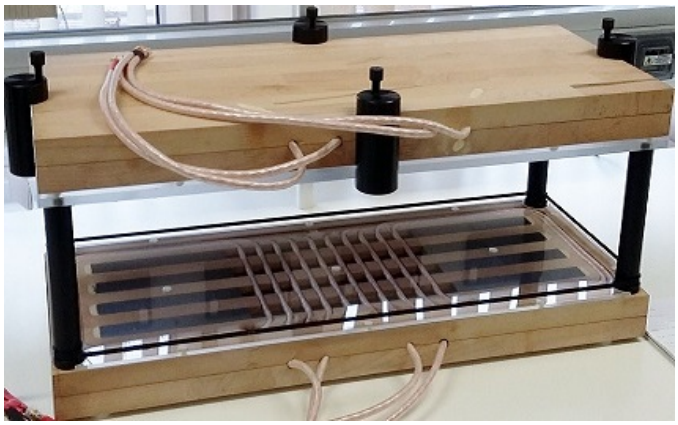

Fig. 4. Photo of constructed full-size WPT pads

The resonant inductor for the primary-side compensation circuit was constructed using a toroidal air-cored design, chosen for reduced losses. The resonant capacitor banks were constructed from an array of series/parallel capacitors, with the number of series and parallel capacitors chosen for low temperature rise at the expected operating point. Capacitors were selected which had a self-resonant frequency significantly

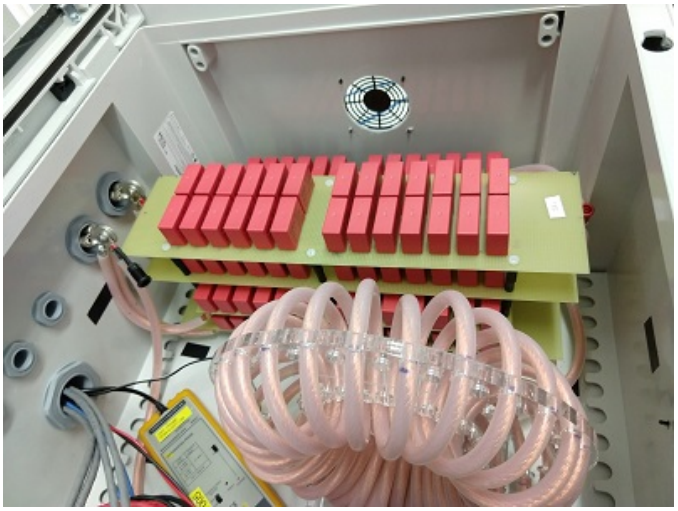

Fig. 5. Photo of resonant circuitry

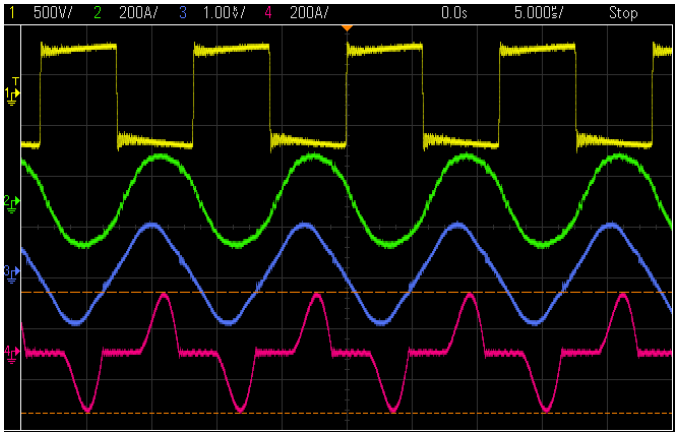

Fig. 6. 50kW results graph (Ch1 = inverter voltage, Ch2 = inverter current, Ch3 = rectifier input voltage, Ch4 = rectifier current)

higher than the operating frequency. The resulting circuit components are shown in Fig. 5.

Initial tests were conducted with a converter made from discrete SiC devices (one device per position on the H-bridge) with good results. Further higher-power testing was conducted using a converter made from SiC power modules (each containing multiple SiC devices in parallel). The power module packaging was an attractive choice from the perspective of inverter construction and thermal management, although some parasitic effects were noticeable during testing.

IV. Tests and Results

For high-power tests the system was assembled in an in-house testing facility with high power DC supplies. The primary side electronics sourced power from a DC power supply and, for simplicity, a large resistor bank was used to provide a load to the DC output of the secondary side electronics. In these tests the converter was controlled to give a full square-wave output and regulation of power was through adjustment of the DC source voltage. Power tests were conducted up to 50 kW (Fig. 6). Near-zero inverter current was successfully achieved at the switching points.

For this test the DC supply was 460 V / 130 A and DC load was 767 V / 69 A. This gives 53 kW of wireless power transferred over a 200 mm gap at a system efficiency of 89 %.

V. Conclusions

A 50 kW WPT system has been designed, built and tested. The system operates over the full gap between the road surface and an EV and utilises a relatively thin module width to assist integration within a vehicle chassis.

The design shows promise and future work will aim to further examine system characteristics and improve system performance. In particular, aspects relating to the thermal performance, tolerance to misalignment, system control and further full-system optimisation will be considered. The current system utilises one module but it is intended that multiple modules could be combined in the future to realise even higher power systems.

References

[1] A. Foote and O. C. Onar, "A review of high-power wireless power transfer," in *2017 IEEE Transportation and Electrification Conference and Expo, ITEC 2017*, 2017.

[2] J. T. Boys and G. A. Covic, "The inductive power transfer story at the University of Auckland," *IEEE Circuits and Systems Magazine*, vol. 15, no. 2, pp. 6–27, 2015.

[3] SAE International, "J2954, Wireless Power Transfer for Light-Duty Plug-In/Electric Vehicles and Alignment Methodology," 2017. [Online]. Available: https://www.sae.org/standards/content/j2954_201711/

[4] M. Budhia, J. T. Boys, G. A. Covic, and C. Y. Huang, "Development of a single-sided flux magnetic coupler for electric vehicle IPT charging systems," *IEEE Transactions on Industrial Electronics*, vol. 60, no. 1, pp. 318–328, 2013.

[5] M. Budhia, G. Covic, and J. Boys, "A new IPT magnetic coupler for electric vehicle charging systems," in *IECON Proceedings (Industrial Electronics Conference)*. IEEE, 2010, pp. 2487–2492.

[6] W. Li, H. Zhao, J. Deng, S. Li, and C. C. Mi, "Comparison Study on SS and Double-Sided LCC Compensation Topologies for EV/PHEV Wireless Chargers," *IEEE Transactions on Vehicular Technology*, vol. 65, no. 6, pp. 4429–4439, 2016.

[7] A. Ramezani, S. Farhangi, H. Iman-Eini, B. Farhangi, R. Rahimi, and G. R. Moradi, "Optimized LCC-Series Compensated Resonant Network for Stationary Wireless EV Chargers," *IEEE Transactions on Industrial Electronics*, vol. 66, no. 4, pp. 2756–2765, 2019.